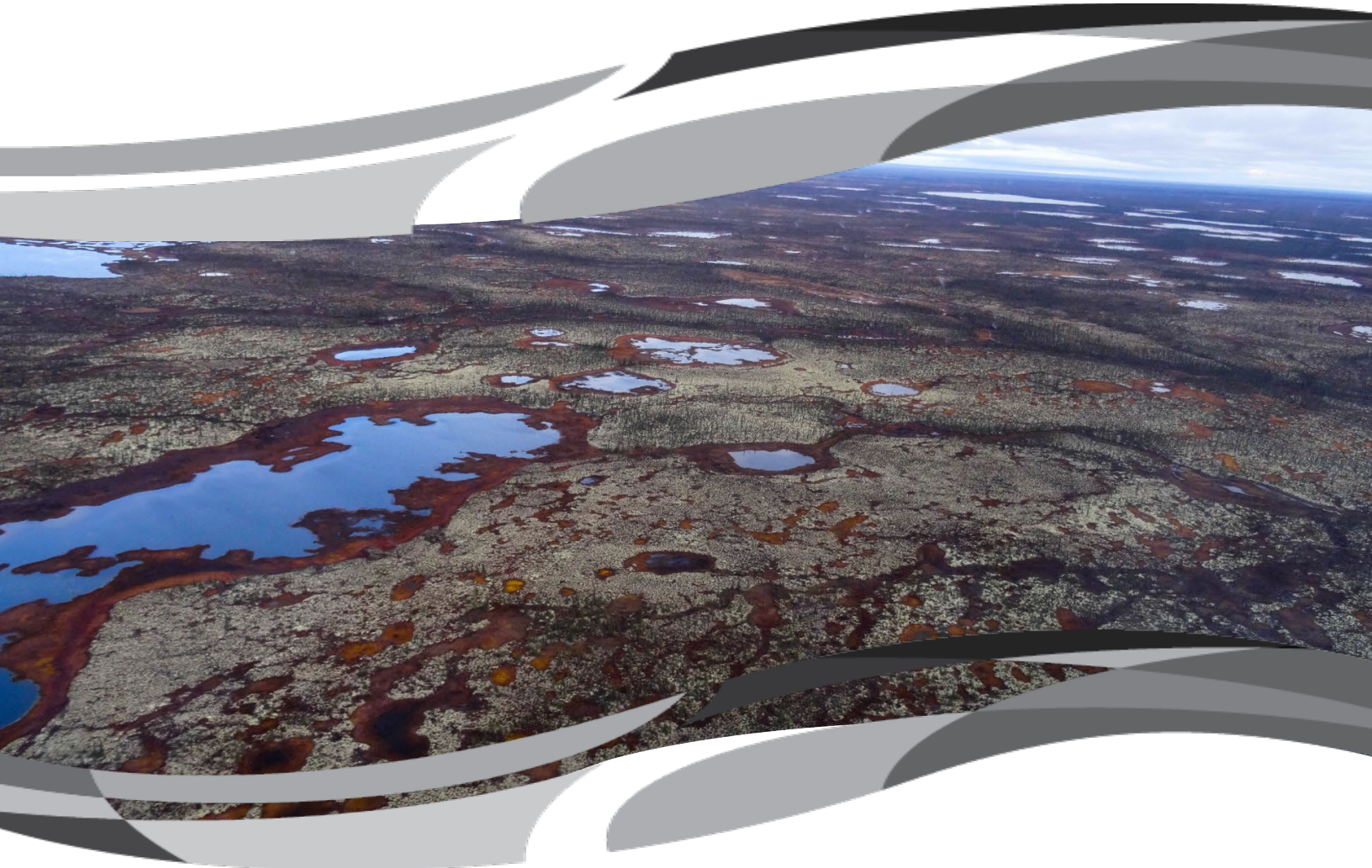**NWT Open Report 2020-010**

**Thermokarst Mapping Collective:
Protocol for organic permafrost terrain and preliminary
inventory from the Taiga Plains test area, Northwest Territories**

C. Gibson, P.D. Morse, J.M. Kelly, M.R. Turetsky, J.L. Baltzer,
T. Gingras-Hill, and S.V. Kokelj

**NORTHWEST TERRITORIES
GEOLOGICAL SURVEY**

Government of
Northwest Territories

NWT Open Report 2020-010

Thermokarst Mapping Collective:
Protocol for organic permafrost terrain and
preliminary inventory from the Taiga Plains test
area, Northwest Territories

Carolyn Gibson [1], Peter D. Morse [2], Jocelyn M. Kelly [1],
Merritt R. Turetsky [1,3], Jennifer L. Baltzer [4], Tristan Gingras-Hill [4], and
Steven V. Kokelj [5]

Carolyn Gibson
University of Guelph
Guelph, Ontario
Email: cgibso04@uoguelph.ca

Steven V. Kokelj
Northwest Territories Geological Survey
Department of Industry, Tourism and Investment
Government of Northwest Territories
Yellowknife, Northwest Territories
Email: steve_kokelj@gov.nt.ca or NTGS@gov.nt.ca

[1] University of Guelph, Guelph, ON
[2] Geological Survey of Canada, Ottawa, ON
[3] Institute of Arctic and Alpine Research, Colorado University, Boulder, CO
[4] Biology Department, Wilfrid Laurier University, Waterloo, ON
[5] Northwest Territories Geological Survey, Yellowknife, NT

i

Abstract

The Northwest Territories Thermokarst Mapping Collective collaboratively develops protocols to map permafrost landforms and evidence of thermokarstto create inventories and assess permafrost terrain sensitivity for the Northwest Territories. This report presents a protocol for mapping organic permafrost terrain in the sporadic and discontinuous permafrost zone using Sentinel-2 satellite imagery, and an inventory of the spatial distribution of organic permafrost terrain (permafrost peatlands) and related thermokarst for a test area in the sporadic and discontinuous permafrost zone of the Taiga Plains, Northwest Territories. A 322 340 km^2 area was mapped using a gridded classification approach with 3.75 km × 3.75 km grid cells (within the 15 km × 15 km grid cells used by the Northwest Territories Thermokarst Collective). Of the 3.75 km × 3.75 km cells, 53% contained permafrost peatland complexes, and the degree of thermokarst degradation decreased abruptly north of 64°N. These preliminary data precede the completion of mapping all of the Northwest Territories, including organic terrain in the continuous permafrost zone.

Introduction

The thawing of ice-rich permafrost ("thermokarst") can reduce ground stability, modify terrain, and reconfigure drainage patterns, affecting terrestrial and aquatic ecosystems (Kokelj and Jorgenson 2013) and present challenges to northern infrastructure and communities (Hjort *et al.* 2018). Identifying geomorphic terrain features indicative of permafrost and thermokarst processes enables mapping and predicting thaw susceptible landscapes (Chasmer and Hopkinson 2017). Variations in geology, topography, climate, and ecosystems yield a diversity of permafrost conditions and controls the response to thaw. However, no empirical or systematic broad-scale dataset describes the variation in thaw sensitivity across the Northwest Territories (NWT). In 2019, the NWT Thermokarst Mapping Collective was initiated to collaboratively develop a set of methodologies to classify and map permafrost terrain and thermokarst features using Sentinel-2 satellite imagery available for the entirety of the NWT. This project implements a grid-based framework to map relevant features on a uniform grid, thus allowing for standardized mapping across large regions.

Organic permafrost terrain is one of the four mapping themes (slopes and mass wasting, hydrological features, periglacial features, and organic terrain) identified by the Collective. The goal of the Organic Terrain Working Group is to determine the distribution of permafrost peatland complexes in the NWT and to categorize the degree to which organic terrain is affected by thermokarst collapse. A complex is defined by the maximum extent of the current permafrost peat plateau and recently degraded areas within it, Figure 1. This report reviews organic permafrost terrain features in discontinuous permafrost, presents a rubric for identifying them on 2016-2017 Sentinel-2 imagery, describes a protocol for mapping the distribution and state of organic permafrost terrain, and presents a preliminary inventory for the Taiga Plains ecoregion underlain by discontinuous permafrost. The preliminary data product in this report precedes the completion of mapping for other ecoregions in the NWT that will use the same rubric and semi-automative approach presented here.

Background

Permafrost and thermokarst

Permafrost, ground that remains at or below 0°C for two or more years (ACGR 1988), is the geological manifestation of climate. In northwestern Canada, the distribution, thickness, thermal regime, and ice content of permafrost reflect the geological legacy of the region and the influence of climatic variations and biophysical processes over the past hundreds to thousands of years (Williams and Smith 1989). Current and past biophysical factors including topography, vegetation cover, snow depth, soil type, and moisture conditions, all have an important influence on defining spatial variation in local and regional permafrost conditions (Williams and Smith 1989; Bonnaventure *et al.* 2012; Carpino *et al.* 2018). For example, seasonal variation in the thermal properties of peat, insulating the ground in the summer and promoting cooling in the winter,

1

explains why permafrost can exist where mean annual air temperatures exceed 2°C (Romanovsky and Osterkamp 1995; Burn 2004). As a result, permafrost is increasingly restricted to peatlands/ organic terrain with decreasing latitude (Brown 1967). At soil temperatures below 0°C, nearly all the water is present as ground ice. For boreal regions permafrost that is in fine-grained, frost-susceptible materials, it is typically ice rich (Mackay 1972; Shur *et al.* 2005). Though related to temperature, the most important determinant of ground ice content is the geomorphic setting, which reflects soil physical properties, available moisture, and the process and duration of ice formation (Mackay 1972).

Permafrost can thaw if climate change or other disturbances, such as a fire (*e.g.,* Burn 1998; Gibson *et al.* 2018) or development (*e.g.,* Hjort *et al.* 2018), alter surface boundary conditions and cause the ground to warm. Degradation of ice-rich permafrost leads to the consolidation of thawed materials and ground subsidence, which in flat terrain may lead to ponding. Ponding has a warming effect on the ground, which is typically compounded by the accumulation of a deeper snow cover in depressions formed by subsidence. Together, ponding and the accumulation of snow produce a feedback that promotes further thaw, *e.g.,* Morse and Burn (2013) and O'Neill and Burn (2017) Ground ice conditions influence the ecological response to thawing permafrost. In particular, discontinuous permafrost has a high spatial variation of frozen and unfrozen terrain, with variable ice content in permafrost-affected areas (Fortier *et al.* 2011). Near-surface permafrost thaw is anticipated to accelerate during the 21st century (Koven *et al.* 2013), due to a projected ~2°C to 4°C increase in global mean surface temperature compounded by a high-latitude amplification factor of 2.2 to 2.4 (Collins *et al.* 2013). This may cause permafrost to thaw entirely in parts of the discontinuous permafrost zone (Zoltai 1993; Chasmer and Hopkinson 2017). Knowledge of permafrost conditions and landscape variation concerning the nature and intensity of thermokarst is critical to predicting landscape and ecosystem change trajectories. However, in the NWT empirical information on permafrost distribution and thermokarst development patterns are limited to regional or local scale studies. This mapping project aims to address this information gap by mapping permafrost terrain and evidence of thermokarst on a territorial scale.

Organic permafrost terrain and related thermokarst

The rates and magnitudes of organic permafrost terrain response to thaw are of particular interest (*e.g.*, Baltzer *et al.* 2014; Chasmer and Hopkinson 2017; Gibson *et al.* 2018) due to the vast amounts of stored carbon and feedbacks on carbon cycling and global climate change (Schuur *et al.* 2008; Schuur and Abbott 2011). In permafrost regions, peat plateaus, polygonal peat plateaus, and palsas (Figure 1) are good indicators of permafrost, and the spatial extent of these features vary based on physiography, climate history, and ecosystem conditions (Zoltai and Tarnocai 1975).

Permafrost peatland complexes are characterized by flat areas of well-drained peat, elevated above surrounding terrain due to the accumulation of organic material and uplift of the terrain that resulted as permafrost aggraded into underlying fine-grained sediments. These landscapes are distinct on air photographs and satellite imagery due to the high reflectance of lichen-covered surfaces and a heterogenous (open) canopy of black spruce forest (*Picea mariana*). These landscapes are perforated with thermokarst collapse scars and/or distinct internal lawns characterized by bogs, fens, and shallow open water wetlands that are permafrost free (Zoltai and

2

Tarnocai 1975; Zoltai 1993; Figure 1a). Some peatland complexes are dissected by troughs that form above a network of ice wedges, creating a polygonal pattern when viewed from above (Zoltai and Tarnocai 1975; Figure 1b). However, these polygonal peatland complexes do not occur within the test area reported here and will be described in more detail and mapped in subsequent reports. This report only concerns permafrost peatlands found within the test area and does not include all organic features found elsewhere within the NWT.
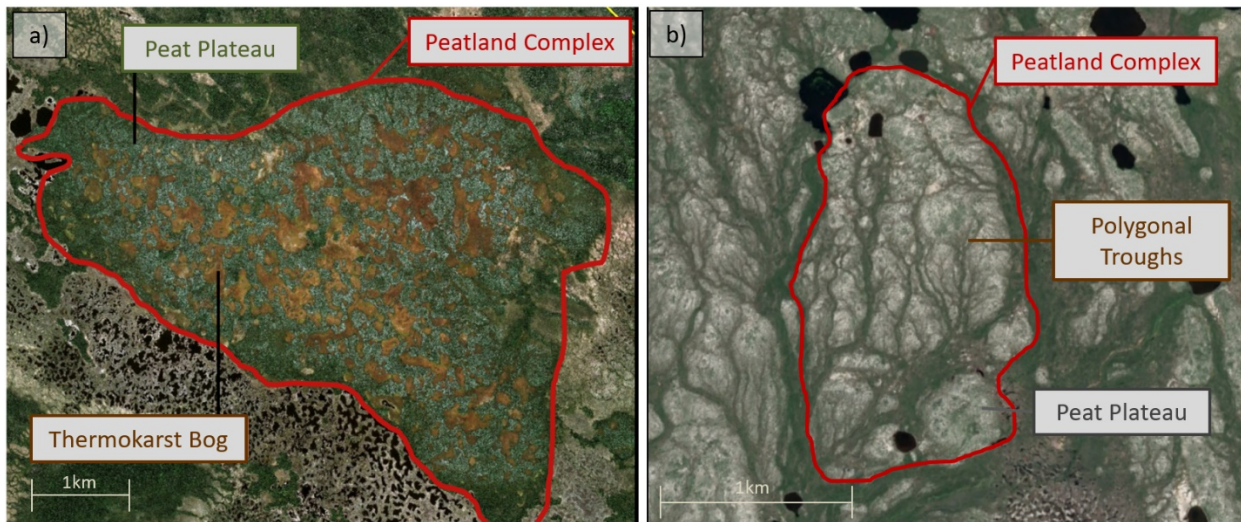

Figure 1. a) Example of permafrost peat plateau complex (61°14'6.79"N, 117°35'23.81"W) in World View 2 imagery. Peat plateaus (medium green with 'salt and pepper' texture) represent areas where the permafrost is intact, while fen and/or bog areas (light to golden brown with comparatively homogeneous texture) are those in which permafrost thaw (thermokarst) has occurred. b) Example of polygonal permafrost peatland (68°1'41.97"N, 132°38'51.45"W) in continuous permafrost in World View 2 imagery. Peat plateaus (white due to lichen coverage) are crisscrossed with polygonal troughs.

Permafrost peatlands, by nature, exist in a state of dynamic equilibrium, undergoing a cycle of permafrost aggradation, degradation, and re-aggradation over about 600-years (Zoltai 1993). During the aggradation phase, the waterlogged conditions in bogs are dominated by *Sphagnum riparium*. This highly productive moss rapidly accumulates biomass, which over time raises the organic surface above the water table. As the surface rises, surface moisture conditions become increasingly dry, and there is a succession of moss species; *Sphagnum riparium* is replaced by *Sphagnum angustifolium*, and then by *Sphagnum fuscum* (Zoltai 1993). At this stage, black spruce (*Picea mariana*) and lichen (*Cladonia* spp.) can establish. The surface organic material is relatively dry in summer, which minimizes ground heating due to poor thermal conductivity of dry moss combined with evapotranspiration. Wetting of the surface organic material, by autumn precipitation, enhances winter ground cooling due to the high thermal conductivity of frozen saturated mosses. As a result, the surface organic layer promotes permafrost formation and preservation (Nelson *et al.* 1985). This "thermal offset" enables equilibrium or aggrading permafrost to exist at locations where the mean annual ground surface temperatures are above 0°C (Burn and Smith 1988). Over time, the permafrost table rises with the accumulation of organic matter, trapping pore water (~80% pore space) in the organic matter as ice, creating a peat plateau

3

with a frozen, icy core (Zoltai 1993). Aggradation of permafrost into the underlying fine-grained mineral soils, and concomitant ice enrichment by segregation, can contribute significantly to the relative elevation of the peat plateau.

Permafrost degradation and thermokarst development are initiated by gradual (e.g., climate change, development of dilation cracks) and/or rapid (e.g., fire) events that modify the ground thermal regime (Zoltai 1993). As thawing progresses, the plateau subsides to the level of the surrounding water table, waterlogging and killing the black spruce (Islam and Macdonald 2004; Baltzer *et al.* 2014). The trajectory of thermokarst subsidence is a function, in part, of the ice content of the underlying mineral sediments. As subsidence continues, the surface soil layer approaches the water table, and *Sphagnum fuscum* is gradually replaced by *Sphagnum angustifolium* then by *Sphagnum riparium* (Gignac *et al.* 1991; Zoltai 1993). If there is sufficient organic accumulation in the thermokarst depression, the organic surface may again rise above the water table, and permafrost may subsequently re-aggrade to complete the cycle (Zoltai 1993). Currently, in the southern NWT, plateaus are thawing and developing thermokarst between a rate of 0.26% and 0.34% per year at undisturbed sites (Chasmer *et al.* 2010; Baltzer *et al.* 2014; Gibson *et al.* 2018), and thermokarst development is three times faster in areas disturbed by fire (Gibson *et al.* 2018). Due to the cumulative impacts of warming and increasing disturbances such as fire activity (Gibson *et al.* 2018) and the sparsity of information on the ice contents of underlying sediments, it is unclear if it is possible for permafrost to re-aggrade in these permafrost peatlands.

Taiga Plains Test Area

The sporadic and discontinuous permafrost zone of the Taiga Plains (excluding Great Bear Lake and Great Slave Lake within) was selected as a test area for peat plateau complex mapping (Figure 2). This region is characterized by a range of permafrost conditions comprising about 21% of the study region and provides an ecoregion-based mapping product. The test area comprises 22 922 grid cells measuring 3.75 km × 3.75 km, totalling 322 340 km². This area is characterized by a subdued relief and gently rolling plains and is underlain with horizontal beds of sedimentary rocks consisting of limestone, shale, sandstone, and conglomerates. The present landscape of the Taiga Plains is primarily a legacy of glaciation of the entire Mackenzie Valley until about ~30 ka BP by the Laurentide Ice sheet, and subsequent impoundment of meltwater to establish glacial lakes during deglaciation (Duk-Rodkin and Lemmen 2000). Most of the test area is within the influence of glacial Lake McConnell, which by about 10 ka BP had become the second-largest Pleistocene lake in North America, covering all of the modern Great Bear, Great Slave and Athabasca basins (Lemmen *et al.* 1994). Sediment deposition accompanied inundation by glacial Lake McConnell between about 12 700 and 9300 cal BP (Lemmen *et al.* 1994). This late-Quaternary history has left a suite of fine-grained surficial deposits, most notably, large areas of glaciofluvial and glaciolacustrine materials and extensive till plains that have yielded extensive, poorly-drained landscapes conducive to organic accumulation and wetland development. Consequently, the Taiga Plains is one of the major peatland regions of Canada – nearly 40% of the study area is peatlands (Ecosystem Classification Group 2007). Peat accumulation in this area was initiated following deglaciation ~9000 years ago (Loisel *et al.* 2014). Soil development in the Taiga Plains is strongly related to the climate and local moisture and drainage conditions, with peat depths varying between

4

2 m and 6 m. Permafrost aggradation began during the climate cooling after the Holocene thermal maximum ~5000 years ago and became more widespread following further cooling 1200 years ago (Pelletier *et al.* 2017).
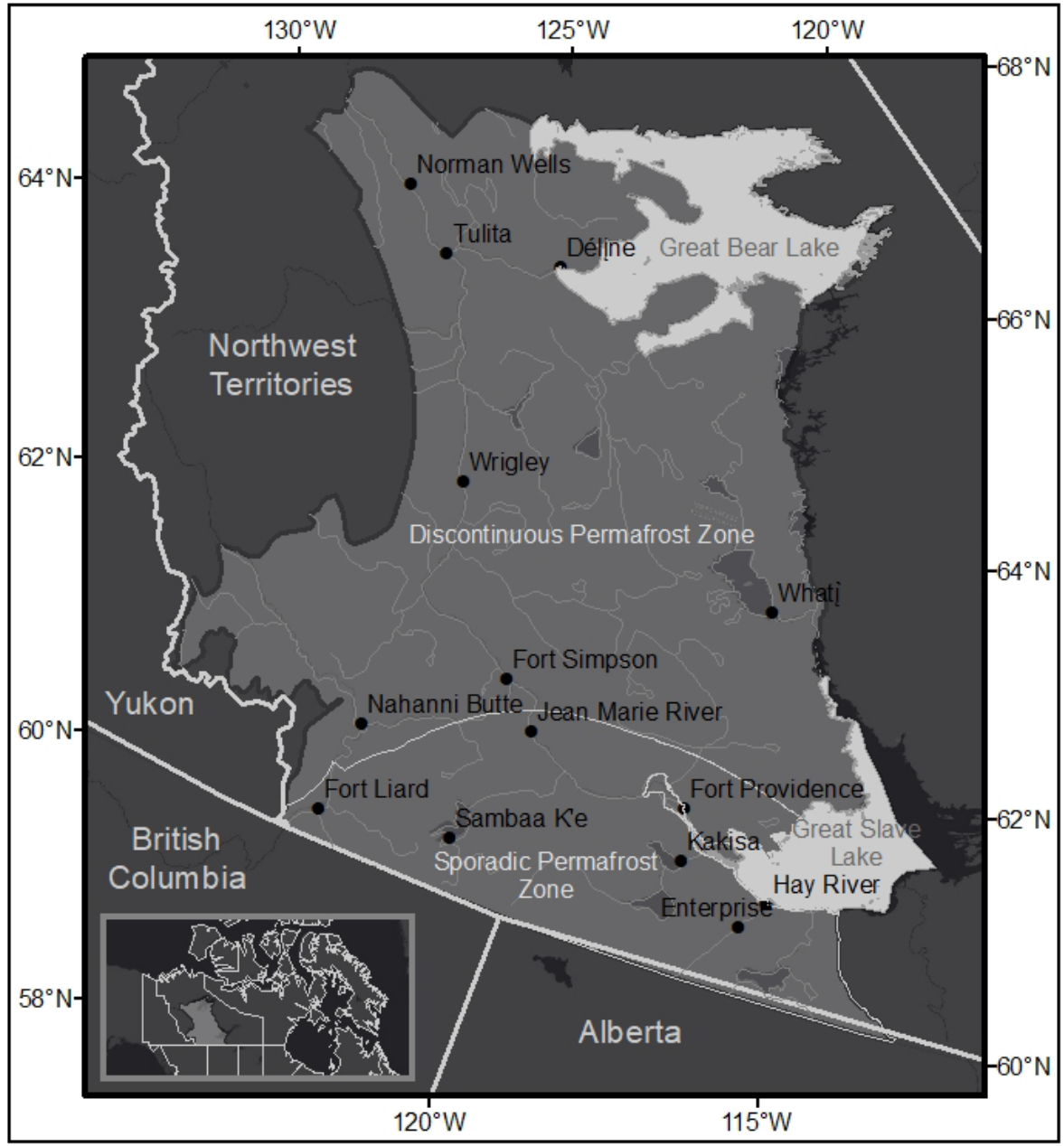

Figure 2. Map of the Taiga Plains test area within the NWT (322 340 km²). The bottom left inset shows the location of the study area relative to northern Canada.

Methodology

Sentinel-2 satellite imagery, processing, and spatial extent

The NWT Thermokarst Mapping Collective is focused on map products derived from an electronic mosaic of Sentinel-2 satellite imagery obtained for the Government of Northwest Territories. The mosaic comprises Sentinel-2 images collected in July and August of 2016 and 2017, to minimize snow and ice cover. Input images were selected to minimize cloud cover, smoke, and haze. Processed Sentinel-2 imagery, provided by Northwest Territories Centre for Geomatics, was produced under a contract issued through a competitive process to Pacific Geomatics© (Victoria, BC). Sentinel-2 data are 10-m resolution, true-color composite (B04 (Red), B03 (Green), B02 (Blue)) and false-colour composite (B08 (NIR), B04 (Red), B03 (Green)) Level 1C imagery, calibrated to Top of Atmosphere Reflectance. The image data coverage extends outside of the NWT to include the watershed areas of major transboundary rivers, including the Liard and Peel watersheds, northward flowing rivers from the Yukon into the Mackenzie Delta and Beaufort Sea, Victoria Island, mainland Nunavut west of longitude 112°W, and northward-flowing rivers from Alberta or Saskatchewan into the NWT, excluding the Peace and Athabasca watersheds (Figure 3). During mapping, the satellite imagery is viewed at a scale between 1:20 000 and 1:30 000 and histogram stretches are applied to the imagery as needed to enhance the contrast.

Area of interest and mapping grid

The general mapping scheme for the NWT thermokarst collective project is to assess the presence or relative abundance of permafrost features defined within 15 km × 15 km areas of interest (AOI). In this way, the entire NWT is categorized into approximately 13 499 AOI tiles organized as rows and columns (Figure 3). For inventorying other permafrost features as part of the mapping initiative (e.g., slope, mass wasting, hydrological, and periglacial features) AOI tiles are subdivided into four 7.5 km × 7.5 km quartiles to facilitate characterization of feature density. Due to the high variability in the distribution of organic permafrost terrain and difficulty in mapping peatlands as "point" features and counts, the grid system is further subdivided into four 3.75 km × 3.75 km sub-quartile cells, producing 16 sub-grid cells per 15 km^2 AOI (Figure 4). The feature assessment includes an estimation of percent extent of organic permafrost terrain within each sub-grid cell. Data in this report is reported at the 3.75 km × 3.75 km sub-quartile cells.

Identifying organic permafrost terrain and associated thermokarst features on Sentinel-2 imagery

Peatland permafrost complexes, including those with polygons, are good indicators of permafrost within discontinuous permafrost (Zoltai and Tarnocai 1975; Figure 1a). This report focuses on methodologies to identify and map organic permafrost terrain within the discontinuous permafrost zone. Polygonal permafrost peatlands will be addressed in a follow-up report for organic terrain in continuous permafrost.

6

Recognizing there is a cyclical collapse and re-establishment of peat plateaus (Zoltai and Tarnocai 1975), it was assumed that current thaw features of the complex delineate the former peat plateau extent. The method developed herein produces areal estimates of permafrost peatland complexes and a rough estimate of the degree to which the peat plateau has degraded (thawed or undergone thermokarst). Capture variation is expected at multiple scales across the NWT, as permafrost peatland complexes vary significantly in the extent of thermokarst due to variation in underlying geology, ground ice conditions, hydrology, ground temperatures, and climate. Rates of peat plateau degradation are not determined as the methods do not include a temporal component.
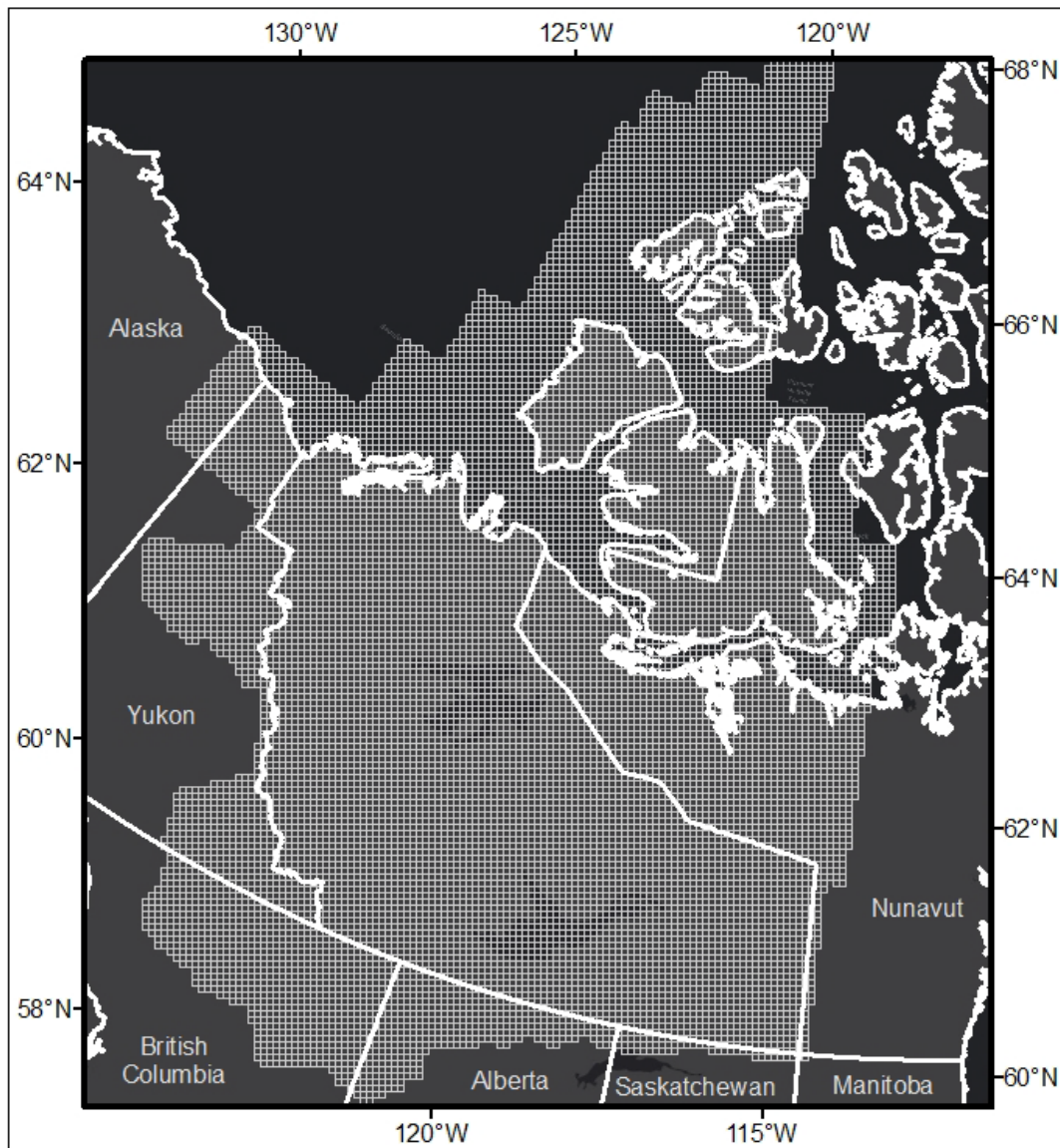
Figure 3. The Thermokarst Collective study area comprises Northwest Territories and shared watershed boundaries. Grids represent 15 km × 15 km areas of interest (AOI).
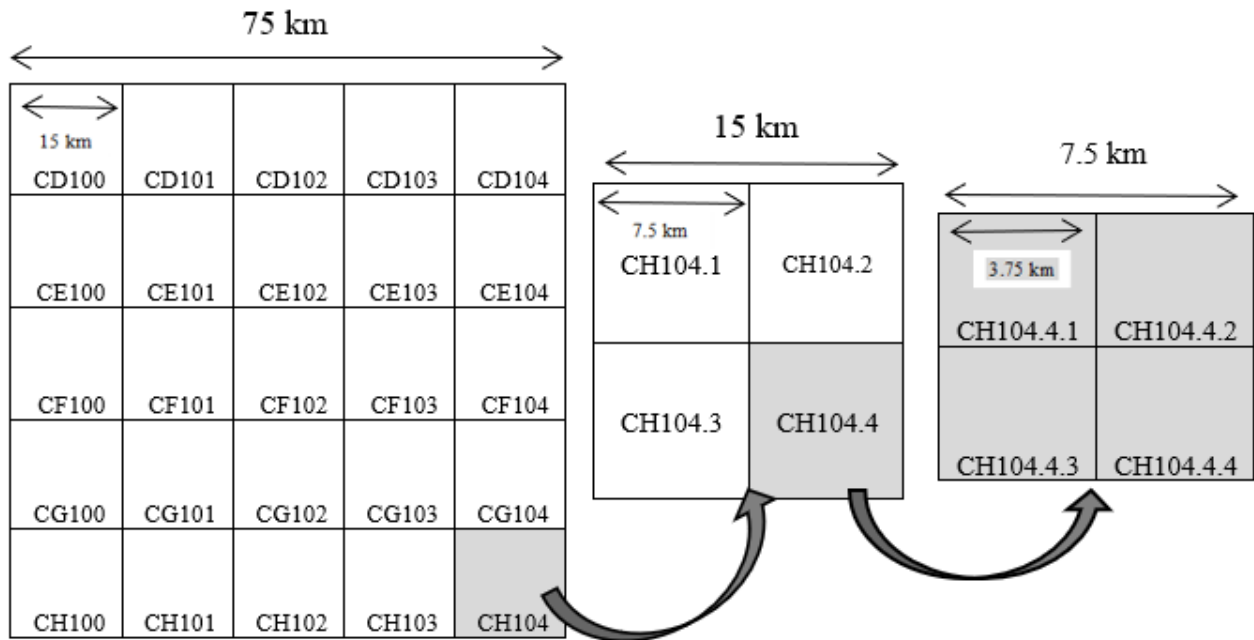
7

Figure 4. Gridded mapping methodology and naming convention. The 15 km × 15 km grid cells were subdivided into 7.5 km × 7.5 km grid cells and then again into 3.75 km × 3.75 km grid cells for mapping organic permafrost terrain.

Identifying peat plateau complexes and percent cover

Several characteristics distinguish peat plateau complexes from the surrounding landscape in Sentinel-2 imagery. All complexes, whether burned/unburned or forested/unforested, typically appear as non-uniform patches that vary in size from less than one kilometre squared to several kilometres squared, with a varying degree of thermokarst in the form of collapse scars (Figure 1a; Figure 5). In contrast, surrounding landscape features such as fens appear as elongated networks, and forested mineral terrain that are not part of a peatland complex should not show thermokarst in the form of collapse scars. Furthermore, these terrains also show a contrasting colour and texture to the organic deposits due to contrasting vegetation and soil moisture conditions. Lakes that are adjacent to, or within, the peatland complex are not considered to be part of the complex. Lakes are larger than thermokarst ponds and typically appear black in true-colour composite Sentinel-2 imagery. In the event of cloud cover, high-resolution imagery from the ArcGIS basemap was used. Lakes and cloud cover are not included in the sub-grid cell area estimate. Examples of percent cover are shown in Figure 5.

The percent cover of the complex within the cell is visually estimated according to the following bins: None (0%), Trace (0% – 2%), Low (3% – 25%), Medium (26% – 50%), High (51% – 75%), Very High (76% – 100%).
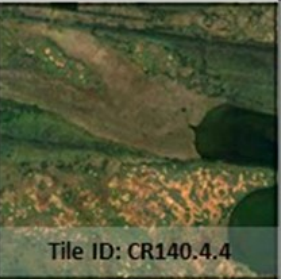
8
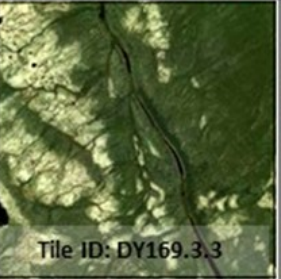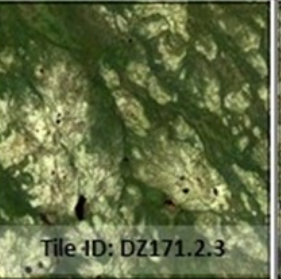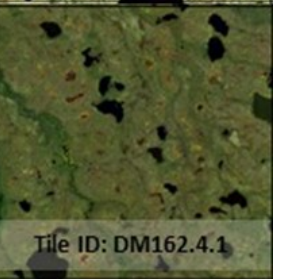
	Negligible (<2%)	Low (2% - 25%)	Medium (26% - 50%)	High (51% - 75%)	Very High (75% - 100%)
Forested Organic Terrain	Tile ID: DC144.1.2	Tile ID: CM141.4.3	Tile ID: CR140.4.4	Tile ID: CZ149.3.3	Tile ID: CK140.3.2
Unforested Organic Terrain	Tile ID: EB172.3.1	Tile ID: EB172.1.3	Tile ID: DY169.3.3	Tile ID: DZ171.2.3	Tile ID: DZ171.4.4
Burned Organic Terrain	Tile ID: CY144.4.4	Tile ID: DF153.3.2	Tile ID: DH152.2.3	Tile ID: DG152.1.3	Tile ID: DM162.4.1

Figure 5. Examples of peat plateau complexes for the suite of mapped attributes: spatial extent, vegetation cover, and fire history.

Forested versus unforested peat plateaus

In true colour composite Sentinel-2 images, peat plateaus and thermokarst areas appear in a variety of colours and textures. Forested peat plateaus are light to medium shades of green, grey, or blueish-green and have a speckled appearance due to the presence of trees that contrast with the underlying lichen-dominated ground cover. Thermokarst features within the forested complex are commonly light to dark in shade and colours vary from reddish-orange, orange, pink, brown, yellow, and beige, and are typically larger than those associated with unforested peat plateau complexes (Figure 6a). Unforested peat plateaus appear to be a relatively homogeneous white due to the lichen-dominated ground cover, while thermokarst features are often black and small relative to the peat plateau area (Figure 6b).
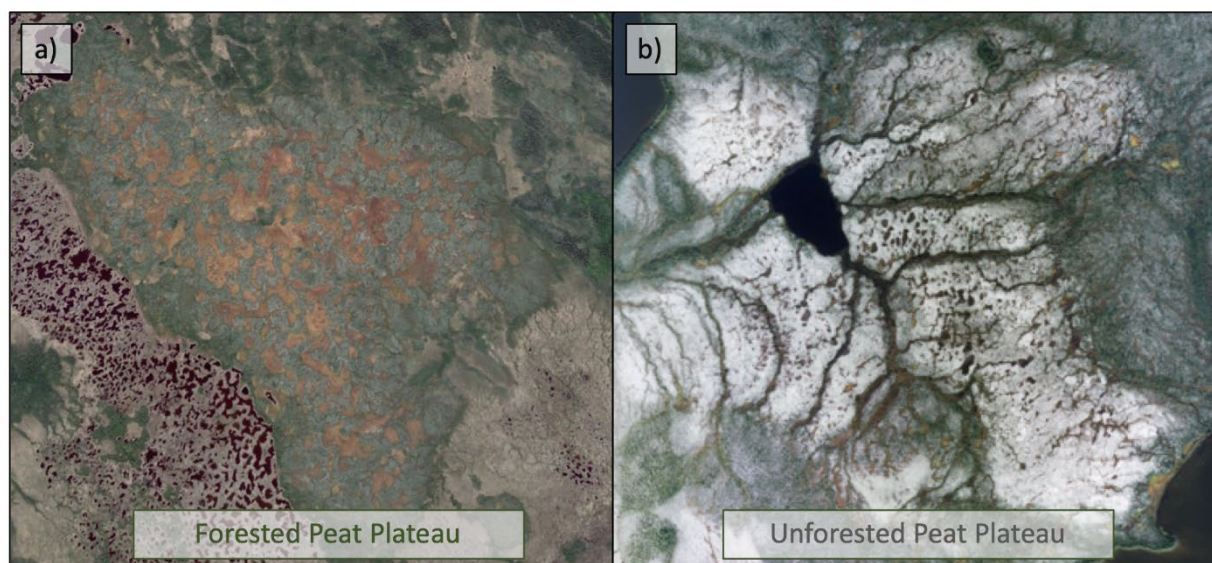
Figure 6. Example of a) a permafrost peatland complex (61°14'6.79"N, 117°35'23.81"W), and b) an unforested permafrost peatland complex (64°53'16.04"N, 126°34'54.18"W).

Fire history

Permafrost peatland complexes affected by wildfire display the same shape and distribution patterns as unburned plateaus, but the colours and textures are different. Recently burned permafrost peatland complexes are black to dark brown (Figure 7a), while older burns are lighter grey to brown (Figure 7b). Comparing the colour of a permafrost peatland complex against the surrounding landscape features and other nearby peatland complexes can help determine whether it has recently burned. Similarly, surrounding unburned peatlands can help to determine if the fire affected peatland is forested or unforested. This method cannot distinguish permafrost peatland complexes that have historically experienced fire and undergone succession (i.e., fire occurred > 50 years ago), as there is often no evidence of older fire disturbance in present-day remotely-sensed imagery. Cells were considered fire affected if more than 50% of the peatland complexes in the cells were affected by fire. This data can be complemented by the Government of Northwest Territories Environment and Nature Resources Fire maps and/or by the Canadian National Fire Database.
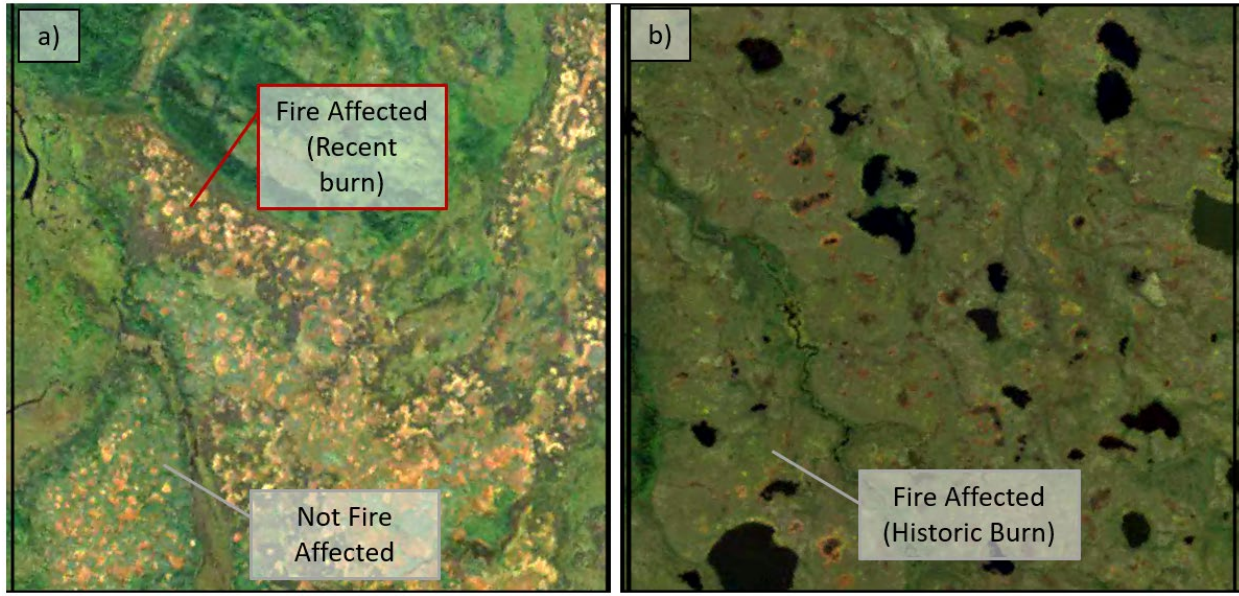
Figure 7. Example for a) recently burned permafrost peatland complex (60°40'44.13"N, 117°41'59.12"W) and b) a historically burned permafrost peatland (Fire year = 2008, 63°29'2.05"N, 120°34'32.51"W). Forested peat plateaus that burned recently are brownish-green, brown to dark brown, or black, while unforested peat plateaus take on a grey colour.

Degree of thermokarst degradation

The degree of peatland degradation was assessed by examining the relative proportion of collapse scar areas within the permafrost peatland complex. Degradation is classified as low (0% – 33%), medium (34% – 66%), or high (67% – 100%). Examples in Figure 8 can be used to guide the assessment.
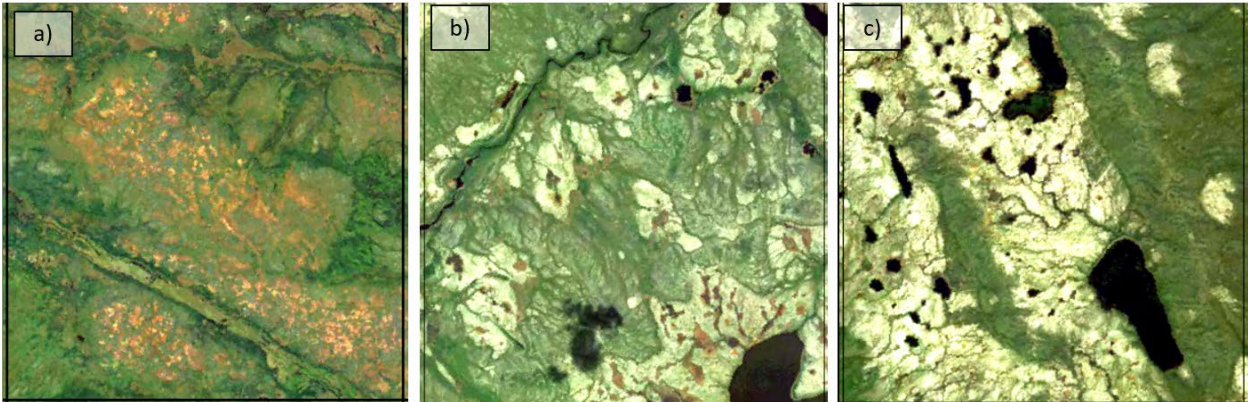
Figure 8. The degree of degradation (thermokarst) is categorized into three categories a) high (67% – 100%, 60°42'25.86"N, 117°52'33.62"W), b) medium (34% – 66%, 63°15'51.34"N, 121°46'44.66"W), and c) low (0% – 33%, 65°19'26.83"N, 124°56'32.56"W).

Populating the dataset

Mapping was conducted within ArcGIS 10.6 using a layer consisting of the 3.75 km × 3.75 km sub-grid cells and a layer showing the Sentinel-2 satellite image mosaic (2016/2017). The Sentinel-2 imagery has a pixel size of 10 m, and features were mapped at a set scale of 1:24 000. This allows mappers to confidently identify organic terrain areas and assess relative coverage within the grid cells. When necessary, ArcGIS World Imagery was used to provide high-resolution interpretations of landscape features or feature validation.

For mapping organic permafrost terrain features, a generalized attribution of recognizable features within every 3.75 km × 3.75 km sub-grid cell of the AOI is used. With the sub-grid cell under investigation centred on the screen, the mapper selects the cell and then the attributes icon on the editor toolbar (once the attribute toolbar appears it remains until closed). The mapper then fills in the editable areas of the attribute table for the selected cell. To standardize the feature attribution (Table 1), fields in the attribute table are populated with a set of predetermined drop-down menus. Assuming most sub-grid cells will not have organic permafrost terrain features, and to make data entry more efficient, the data table is populated with 0 ("Null/None") if the user only fills in their initials.

Once a cell is finished and all attributes are assigned, the border of the cell becomes red and the mapper moves to the next unassessed sub-grid cell.

Table 1. Attributes and inputs for the sub-grid cell classification of peat plateau complexes.

Attribute	Description
Peatland complex area	None (0%), Negligible (< 2%), Low (2% – 25%), Medium (26% – 50%), High (51% – 75%), and Very High (76% – 100%) This attribute is represented by the median of each of these bins within the data frame.
Vegetation type	Null (no permafrost peatland in grid cell), Forested, and Unforested.
Fire history	Null (no permafrost peatland in grid cell), Burned, and Unburned (referring to the organic terrain area, considered unburned if fire did not affect the peatland complex).
Degree of degradation	Null (no permafrost peatland in grid cell), Low, Medium, and High.
Mapper	Initials

For each sub-grid cell, the mapper determines the percent area of the cell (not the land area) containing a permafrost peatland complex and assigns descriptive attributes according to vegetation type, fire history, and degree of degradation (thermokarst). For quality control purposes, the initials of the mapper is also recorded.

12

Though not completed as part of this report, the data are collected and formatted to allow comparison and integration with other datasets developed as a part of the Thermokarst Mapping Collective. Spatial statistics within each 7.5 km × 7.5 km quartile are assigned according to the permafrost peatland complex area. For each quartile, the average percent area covered by a peat plateau complex ($\underline{x}$) is determined from the mean of grouped data from the sub-grid cells:

$$\bar{x} = \frac{\Sigma(fm)}{n} \qquad [1]$$

where m is the midpoint of the class bin (Table 2), f is the frequency of observations in each class, and $n = \Sigma f$ (the sum of all observations in the quartile).

Table 2. Sub-grid cell permafrost peatland complex area bins and midpoints.

Plateau complex area bin (%)	Plateau complex area mid point (%)
Null	Null
0 – 2	2
3 – 25	12.5
26 – 50	37.5
51 – 75	62.5
76 – 100	87.5

The area of permafrost peatland complex can be calculated using the information from Table 2 and Equation 1. For example, using the data shown in Table 3, the aggregate percent area in quartile DQ163.4 is:

$$\underline{x} = \frac{(1 \times 37.5\%) + (3 \times 62.5\%)}{4} = \frac{225\%}{4} = 56.25\%$$

The secondary conditions within the quartile are aggregated according to the percent peatland complex area. For example, only two of the sub-grid cells in quartile DQ163.4 were forested; thus, the amount of forested permafrost peatland complex is:

$$\underline{x} = \frac{(2 \times 62.5\%)}{4} = \frac{125\%}{4} = 31.25\%$$

And the amount of unforested permafrost peatland complex in DQ163.4 is:

$$\underline{x} = \frac{(1 \times 37.5\%) + (1 \times 62.5\%)}{4} = \frac{100\%}{4} = 25\%$$

Similar calculations can be carried out to aggregate results to the Quartile-grid cell for the remaining permafrost peatland complex attributes – degree of degradation and fire history.

13

Table 3. Mapping results for sub-grid cell DQ163.

AOI cell name	Cell number	Quartile-grid cell name	Sub-grid cell name	Peatland complex area (%)	Degree of degradation	Vegetation type	Fire history
DQ163	24227	DQ163.4	DQ163.4.3	62.5	Medium	Forested	Unburned
DQ163	24227	DQ163.4	DQ163.4.1	62.5	Low	Forested	Unburned
DQ163	24227	DQ163.4	DQ163.4.4	62.5	Medium	Unforested	Burned
DQ163	24227	DQ163.4	DQ163.4.2	37.5	Low	Unforested	Unburned

Results

Taiga Plains Test Area Results

In the test area (22 922 grid cells, 3.75 km × 3.75 km), 53% of the 3.75 km × 3.75 km sub-grid cells contained permafrost peatland complexes (Figure 9a). Additionally, 16% of sub-grid cells were classified as negligible, 21% low, 9% medium, 5% high, and 2% very high (Table 4). Of the cells that contained permafrost peatlands, 58% were forested and 42% were unforested. A total of 28205 grid cells contained permafrost peatland complexes recently impacted by fire. Data is also presented as 7.5 km × 7.5 km grid cells to complement mapping efforts of other periglacial features (Figure 9b). There were no significant changes in broadscale patterns of permafrost peatland distributions between the 3.75 km × 3.75 km and 7.5 km × 7.5 km grid cells.

The degree of degradation varied across a latitudinal and elevation gradient within the study area (Figure 10). The degree of degradation also decreases in the centre near Fort Simpson due to the horn plateau which is raised >300 m around the surrounding area.

Table 4: Estimated extent (number of grid cells) of permafrost peatland complex in total, forested, and unforested landscapes (total n=12 177).

	Estimated number of grid cells containing permafrost peatland complexes					
	None	Negligible	Low	Moderate	High	Very high
Forested	8153	2392	2943	1562	908	348
Unforested	4024	1402	1834	516	213	59
Total	12 177	3794	4777	2078	1121	407

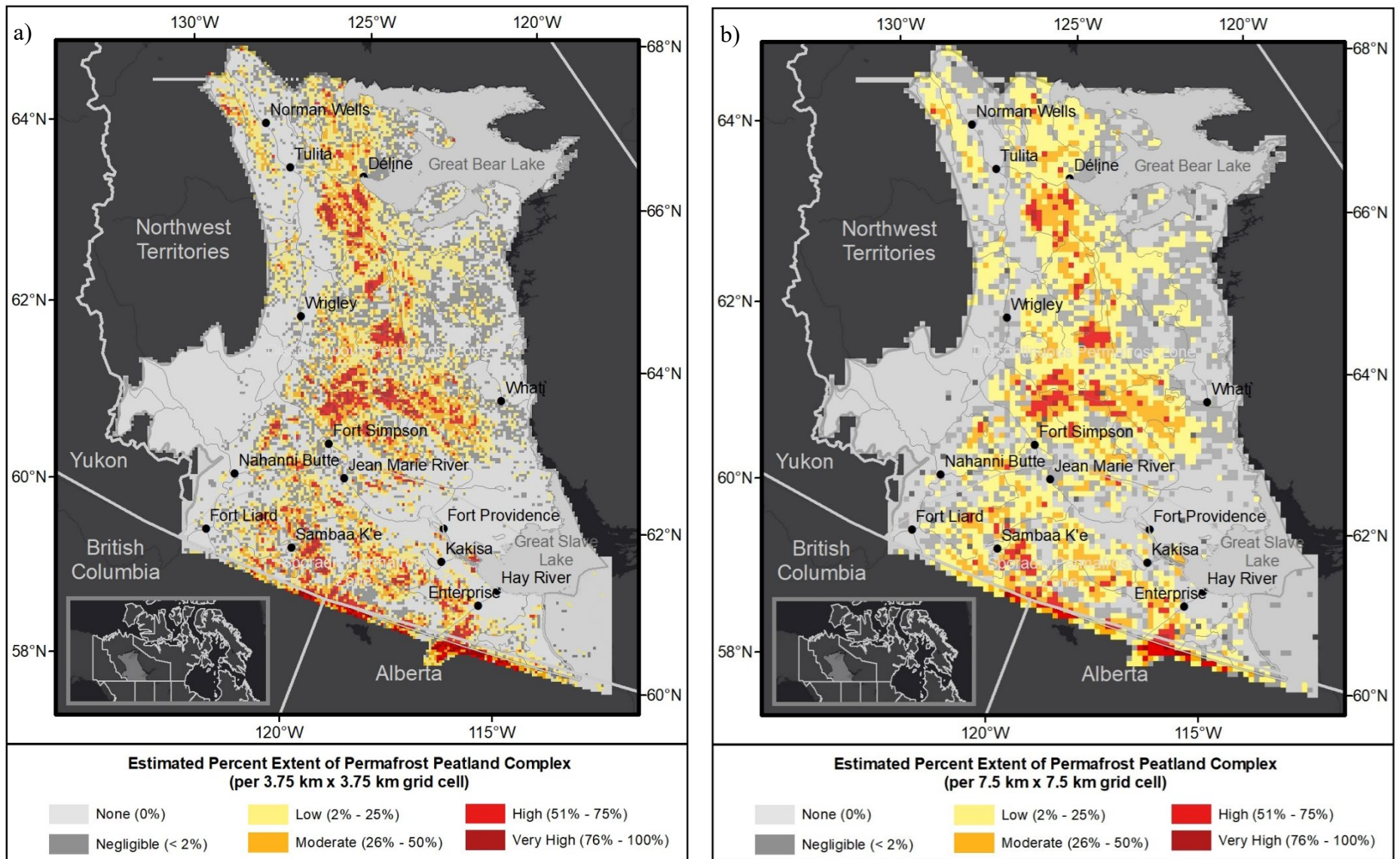Figure 9. Density distribution of peat plateau complexes in the discontinuous permafrost zone of the Taiga Plains. Data are shown according to both a) sub-grid cell size (3.75 km × 3.75 km) and b) grid cell size (7.5 km × 7.5 km).
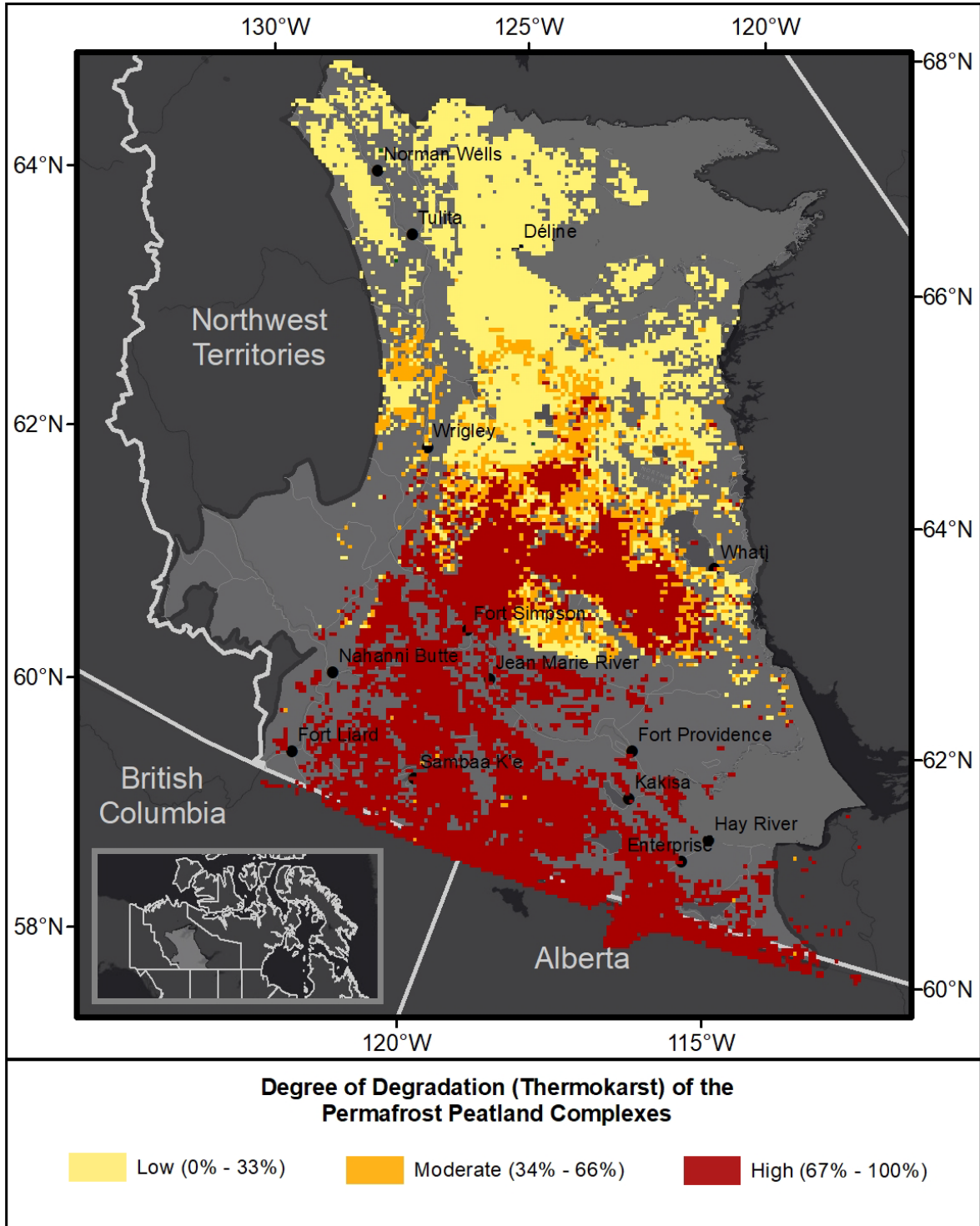
15

Figure 10. Degree of degradation (thermokarst) of the permafrost peatland complexes. Visually estimated as low (0% – 33%), moderate (34% – 67%), or High (67% – 100%).

Quality assessment

A subset of 1185 randomly selected sub-grid cells (~5% of the mapped area) was assessed by two mappers to test the guidelines on interpretation and the accuracy of the approach. The mapper accuracy for percent area estimates is 89% (Table 5). The $\hat{k}$ statistic, a measure of the difference between the actual agreement between the two assessments and the chance agreement between the two, given as:

$$\hat{k} = \frac{\sum_{i=1}^{r} x_{ii} - \sum_{i=1}^{r}(x_{i+} \cdot x_{+i})}{N^2 - \sum_{i-1}^{r}(x_{i+} \cdot x_{+i})}$$
[2]

where r is the number of rows in the error matrix, x_{ii} is the number of observations in row i and column i, x_{i+} is the total of observations in row i, x_{+i} is the total of observations in column i, and N is the total number of observations included in the matrix. For the assessment presented in Table 5, $\hat{k}$ is 0.84, that is, the overall agreement is 84% better than a chance agreement.

Table 5. Error matrix resulting from estimating percent extent of peat plateau complex in randomly sampled sub-grid cells (3.75 km × 3.75 km). Bins are estimates of percent cover.

		Mapper: CG						
		0%	< 2%	2% - 25%	25% - 50%	50% - 75%	75% - 100%	Row Total
	0%	8	30	7	0	0	0	555
	< 2%	20	180	14	1	0	0	215
	2% - 25%	8	23	162	5	0	1	199
Mapper: JK	25% - 50%	0	0	15	106	6	0	127
	50% - 75%	0	0	1	2	58	2	63
	75% - 100%	0	0	0	0	0	22	22
	Column Total	546	233	199	114	64	25	1181

CG's Accuracy

0% = 518/546 = 95%
< 2% = 180/233 = 77%
2% − 25% = 162/199 = 81%
25% − 50% = 106/114 = 93%
50% − 75% = 58/64 = 91%
75% − 100% = 22/25 = 88%

JK's Accuracy

0% = 518/555 = 93%
< 2% = 180/215 = 84%
2% − 25% = 162/199 = 81%
25% − 50% = 106/127 = 83%
50% − 75% = 58/63 = 92%
75% − 100% = 22/22 = 100%

Overall accuracy = (518 + 180 + 162 + 106 + 58 + 22)/1181 = 89%

There was an 85% alignment of the permafrost peatland type (forested/unforested), with the largest misalignment occurring in mid-latitude regions as forested peatlands transition to unforested peatlands. There was a 90% agreement in assigning burned/unburned for fire history. There was an overall 90% agreement in the degree of degradation with a 94% agreement for high, 92% agreement for low, and a 42% agreement for medium. The low agreement on the medium degree of degradation could ~~be a~~ result from the broad category range making it difficult to decipher at the upper and lower ends of the bin range.

Limitations

Data

The primary data limitation is resolution (10-m pixel resolution), which limits the mapping scale (1:24 000). Higher resolution image data are required to resolve the other organic permafrost terrain types. However, though higher resolution data are available, there is a substantial increase in the time and cost to use it for mapping. For the present purpose, the Sentinel-2 data are deemed adequate.

Mapping

There is an inability to map other types of organic permafrost terrain and several limitations were encountered during mapping. The first and most basic was human error during the feature identification and digitization stage. This was minimized by having mappers use the same feature identification criteria to standardize identification and digitization of features. In addition, all feature digitization was evaluated by more than one mapper. Lastly, the generation of attribute data was automated through drop-down lists to reduce human error at the attribute input level.

The second mapping limitation encountered was where the ground was obscured due to cloud cover or shadow. Cloud cover was minimized by obtaining only those images with less than 10% cloud cover. Additionally, shadows can obscure the ground making it difficult to delineate features. However, shadows were generally limited to areas of high relief such as the Richardson and Mackenzie mountains and were not a problem for organic terrain mapping in this report.

The third limitation of mapping is the spatial accuracy of the features being mapped in the imagery, which stems from the orthorectification of the imagery, therefore associated digitized features may not represent the actual geographic position of the feature on the ground.

The fourth, the mapping was carried out mainly as a desktop study. Therefore, limited field verification has been conducted. Features were identified primarily using the Sentinel-2 imagery. However, the use of supplementary data sources (Google Earth or ArcGIS Earth) were used to compensate for the lack of field verification. In addition, expert knowledge was sought from individuals who had been in the field and have worked on these types of features.

Finally, the mapping was carried out only for a subset of the NWT within one ecological district and only within sporadic and discontinuous permafrost. This test area allowed an initial evaluation of the permafrost peatland complex mapping scheme and refinement, but the evaluation is limited to discontinuous permafrost terrain (in boreal forest), where permafrost landscapes and thermokarst features are likely to evolve differently to thaw than other permafrost zones due to contrasting geological, ground ice, ecological and climate conditions, and variation in disturbance regimes. The resulting data defines the distribution of permafrost peatlands throughout the Taiga Plains region of the NWT and the degree to which thermokarst degradation has affected these environments. This product

represents phase 1 of mapping organic terrain distribution and thermokarst effects around 33 NWT communities and then over the entire NWT.

Digital Data

The output of the peat plateau complex mapping is presented in NWT Open Report 2020-010 as georeferenced ArcGIS™ Geodatabase format and Shapefile format files. Metadata, included as an XML file, are annotated in this reports affiliated Appendix.

Summary

This report summarizes the methodology to map discontinuous organic permafrost terrain and to assess the degree of thermokarst degradation in the NWT using Sentinel-2 satellite images and a uniform grid approach to standardize the mapping. The methodology is tested using the area corresponding to the sporadic and discontinuous region of the Taiga Plains ecoregion. Presently, geospatial products that support the prediction of the extent of permafrost features or terrain vulnerability to permafrost thaw are either fine scale products that are restricted in extent (Steedman *et al.* 2016) or cover a large region but have a low resolution (Olefeldt *et al.* 2016) and are not suitable for regional land use planning and risk assessment. The data presented here represent a significant improvement compared to data previously used for mapping organic terrain in permafrost environments, as it provides empirically derived fine-scale data over a large spatial extent. The data presented here can also be aggregated with other gridded mapping of permafrost features to support a comprehensive understanding of permafrost features and thaw sensitive terrain across the NWT.

Acknowledgements

Disclaimer

This document has been created through the joint contribution of the Northwest Territories Geological Survey (NTGS), Government of Northwest Territories (GNWT) and a third party contributor. It is provided for informational purposes only. It does not contain any warranties, representations, or quality commitments, whether expressed or implicit, nor does it contain any guarantees regarding the correctness, integrity, and quality of the information. The NTGS has exercised all reasonable care in the compilation, interpretation, and production of this document and the information has been obtained from sources that the NTGS believes to be reliable. However, it is not possible to ensure complete accuracy, and all persons who rely on the information contained herein do so at their own risk. The NTGS, the GNWT nor the third party contributor accept liability for any errors, omissions, or inaccuracies that may be included in, or derived from, this document. In no event will the NTGS, the GNWT, the third party contributor nor any of their respective successors, assigns, agents or employees be held liable in any way for damages suffered, direct or indirect, as a result of any action or inaction taken in reliance on information provided herein.

Terms of use

All rights in this publication are reserved. Use of any data, graphs, tables, maps or other products obtained through this publication, whether direct or indirect, must be fully acknowledged and/or cited. This includes, but is not limited to, all published, electronic or printed documents such as articles, publications, internal reports, external reports, research papers, memorandums, news reports, radio or print.

References

Associate Committee on Geotechnical Research (ACGR), 1988. Canadian Glossary of Permafrost and Related Ground-ice Terms; National Research Council of Canada, Technical Memorandum No. 142, Ottawa, Ontario, 156 pages.

Baltzer, J.L., Veness, T., Chasmer, L.E., Sniderhan, A.E., and Quinton, W.L., 2014. Forests on thawing permafrost: fragmentation, edge effects, and net forest loss; Global change biology, volume 20, pages 824–834. https://doi.org/10.1111/gcb.12349

Bonnaventure, P.P., Lewkowicz, A.G., Kremer, M., and Sawada, M.C., 2012. A permafrost probability model for the South Yukon and Northern British Columbia, Canada; Permafrost and Periglacial Processes, volume 23, pages 52-68. https://doi.org/10.1002/ppp.1733

Brown, R.J.E., 1967. Permafrost in Canada; Geological Survey of Canada, National Research Council of Canada, Map 1246a, Ottawa, Ontario.

Burn, C.R., 1998. The response (1958-1997) of permafrost and near-surface ground temperatures to forest fire, Takhini River valley, southern Yukon Territory; Canadian Journal of Earth Sciences, volume 35, pages 194-199. https://doi.org/10.1139/e97-105

Burn, C.R., 2004. The thermal regime of cryosols. *In* Cryosols: Permafrost-affected Soils, Kimble, J.M. (ed.). Springer-Verlag, Berlin, Germany; pages 391-413.

Burn, C R., and Smith, C.A.S., 1988. Observations of the "thermal offset" in near-surface mean annual ground temperatures at several sites near Mayo, Yukon Territory, Canada; Arctic, volume 41, pages 99-104.

Canadian National Fire Database: https://cwfis.cfs.nrcan.gc.ca/ha/nfdb

Carpino, O.A., Berg, A., Quinton, W.L., and Adams, J.R., 2018. Climate change and permafrost thaw-induced boreal forest loss in northwestern Canada; Environmental Research Letters, volume 13. https://doi.org/10.1088/1748-9326/aad74e

Chasmer, L., Hopkinson, C., and Quinton, W., 2010. Quantifying errors in discontinuous permafrost plateau change from optical data, Northwest Territories, Canada: 1947- 2008; Canadian Journal of Remote Sensing, volume 36, pages 211–223. https://doi.org/10.5589/m10-058

Chasmer, L.E., and Hopkinson, C., 2017. Threshold loss of discontinuous permafrost and landscape evolution; Global Change Biology, volume 23, pages 2672-2686. https://doi.og/10.1111/gcb.13537

Collins, M., Knutti, R., Arblaster, J., Dufresne, J.-L., Fichefet, T., Friedlingstein, P., Gao, X., Gutowski, W.J., Johns, T., Krinner, G., Shongwe, M., Tebaldi, C., Weaver, A.J., and Wehner, M., 2013. Long-term Climate Change: Projections, Commitments and Irreversibility. *In* Climate Change 2013: The Physical Science Basis, Cambridge University Press, Cambridge, United Kingdom and New York, New York, United States, pages 1029-1136.

Duk-Rodkin, A., and Lemmen, D.S., 2000. Glacial history of the Mackenzie region. I*n* The Physical Environment of the Mackenzie Valley, Northwest Territories: a Base Line for the Assessment of Environmental Change, L.D. Dyke and G.R. Brooks (eds.); Geological Survey of Canada, Bulletin 547, pages 11-20.

Ecosystem Classification Group. Ecological Regions of the Northwest Territories – Taiga Plains. (Department of Environment and Natural Resources, Government of the Northwest Territories, Yellowknife, 2007).

Fortier, R., LeBlanc, A.-M., and Wenbing, Y., 2011. Impacts of permafrost degradation on a road embankment at Umiujaq in Nunavik (Quebec), Canada; Canadian Geotechnical Journal, volume 48, pages 720-740. https://10.1139/t10-101

Gibson, C.M., Chasmer, L.E., Thompson, D.K., Quinton, W.L., Flannigan, M.D., and Olefeldt, D., 2018. Wildfire as a major driver of recent permafrost thaw in boreal peatlands; Nature Communications, volume 9. https://doi.org/10.1038/s41467-018-05457-1

Gignac, L.D., Vitt, D.H., Zoltai, S.C., and Bayley, S.E., 1991. Bryophyte response surfaces along climatic, chemical, and physical gradients in peatlands of Western Canada; Nova Hedwigia, volume 93, pages 29–45. https://doi.org/10.1007/BF00044922

Hjort, J., Karjalainen, O., Aalto, J., Westermann, S., Romanovsky, V.E., Nelson, F.E., Etzelmüller, B., and Luoto, M., 2018. Degrading permafrost puts Arctic infrastructure at risk by mid-century; Nature Communications, volume 9. https://doi.org/10.1038/s41467-018-07557-4

Islam, M.A., and Macdonald, S.E., 2004. Ecophysiological adaptations of black spruce (Picea mariana) and tamarack (Larix laricina) seedlings to flooding; Trees—Structure and Function, volume 18, pages 35–42. https://doi.org/10.1007/s00468-003-0276-9

Kokelj, S.V., and Jorgenson, M.T., 2013. Advances in Thermokarst Research; Permafrost and Periglacial Processes, volume 24, pages 108–119. https://doi.org/10.1002/ppp.1779

Koven, C.D., Riley, W.J., and Stern, A., 2013. Analysis of permafrost thermal dynamics and response to climate change in the CMIP5 Earth system models; Journal of Climate, volume 26, pages 1977-1900. https://doi.org/10.1175/JCLI-D-12-00228.1

Lemmen, D.S., Duk-Rodkin, A., and Bednarski, J.M., 1994. Late glacial drainage systems along the northwest margin of the Laurentide Ice sheet; Quaternary Science Review, volume 13, pages 805-828. https://doi.org/10.1016/0277-3791(94)90003-5

Loisel, J., Yu, Z., Beilman, D.W., Camill, P., Alm, J., Amesbury, M.J., Anderson, D., Andersson, S., Bochicchio, C., Barber, K., Belyea, L.R., Bunbury, J., Chambers, F.M., Charman, D.J., De Vleeschouwer, F., Fialkiewicz-Koziel, B., Finkelstein, S.A., Galka, M., Garneau, M., Hammarlund, D., Hinchcliffe, W., Holmquist, J., Hughes, P., Jones, M.C., Klein, E.S., Kokfelt, U., Korhola, A., Kuhry, P., Lamarre, A., Lamentowicz, M., Large, D., Lavoie, M., MacDonald, G., Magnan, G., Makila, M., Mallon, G., Mathijssen, P., Mauquoy, D., McCarroll, J., Moore, T.R., Nichols, J., O'Reilly, B., Oksanen, P., Packalen, M., Peteet, D., Richard, P.J.H., Robinson, S., Ronkainen, T., Rundgren, M., Sannel, A.B.K., Tarnocai, C., Thom, T., Tuittila, E-S., Turetsky, M., Valiranta, M., van der Linden, M., van Geel, B., van Bellen, S., Vitt, D., Zhao, Y., and Zhou, W., 2014. A database and synthesis of northern peatland soil properties and Holocene carbon and nitrogen accumulation; Holocene, volume 24, pages 1028–1042. https://doi.org/10.1177/0959683614538073

Mackay, J.R.., 1972. The world of underground ice; Annals of the Association of American Geographers, volume 62, pages 1-22. https://doi.org/10.1111/j.1467-8306.1972.tb00839.x

Morse, P.D., and Burn, C.R., 2013. Field observations of syngenetic ice wedge polygons, outer Mackenzie Delta, western Arctic coast, Canada; Journal of Geophysical Research Earth Surface, volume 118, pages 1320-1332. https://doi.org/10.1002/jgrf.20086

Nelson, F., Outcalt, S.I., Goodwin, C.W., and Hinkel, K.M., 1985. Diurnal thermal regime in a peat covered palsa, Toolik Lake, Alaska; Arctic, volume 38, pages 310-315. https://doi.org/10.14430/arctic2150

O'Neill, H.B., and Burn, C.R., 2017. Impacts of variation in snow cover on permafrost stability, including simulated snow management, Dempster Highway, Peel Plateau, Northwest Territories; Arctic, volume 3, pages150-178. https://doi.org/10.1139/AS-2016-0036

Olefeldt, D., Goswami, S., Grosse, G., Hayes, D., Hugelius, G., Kuhry, P., Romanovsky, V.E., Sannel, A.B.K., Schuur, E.A.G., and Turetsky, M.R., 2016. Circumpolar distribution and carbon storage of thermokarst landscapes; Nature Communications, volume 7, pages 1–11. https://doi.org/10.1038/ncomms13043

Pelletier, N., Talbot, J., Olefeldt, D., Turetsky, M., Blodau, C.,Sonnentag, O., and Quinton, W.L., 2017. Influence of Holocene permafrost aggradation and thaw on the paleoecology and carbon storage of a peatland complex in northwestern Canada; Holocene, volume 27, pages 1391–1405. https://doi.org/10.1177/0959683617693899

Romanovsky, V.E., and Osterkamp, T.E., 1995. Interannual variations of the thermal regime of the active layer and near surface permafrost in Northern Alaska; Permafrost and Periglacial Processes, volume 6, pages 313-335. https://doi.org/10.1002/ppp.3430060404

Sentinel-2 Data Moasic: https://sentinel.esa.int/web/sentinel/missions/sentinel-2

Shur, Y.L., and Hinkel, K.M., and Nelson, F.E., 2005. The transient layer: implications for geocryology and climate science; Permafrost and Periglacial Processes, volume 16, pages 5-17. https://doi.org/10.1002/ppp.518

Schuur, E.A.G., and Abbott, B., 2011. High risk of permafrost thaw; Nature, volume 480, pages 32-33. https://doi.org/10.1038/480032a

Schuur, E.A.G., Canadell, J.G., Goryachkin, S.V., Kuhry, P., Shiklomanov, N., Lafleur, P.M., Rinke, A., Hagemann, S., Vogel, J.G., Romanovsky, V.E., Mazhitova, G., Tarnocai, C., Lee, H., Bockheim, J., Nelson, F.E., Field, C.B., Euskirchen, E., Schuur, E.A.G., Zimov, S.A., and Venevsky, S., 2008. Vulnerability of Permafrost Carbon to Climate Change: Implications for the Global Carbon Cycle; BioScience, volume 58, pages 701–714. https://doi.org/10.1641/B580807

Steedman, A.E., Lanz, T.C., and Kokelj, S.V., 2016. Spatio-temporal variation in high-centre polygons and ice-wedge; Permafrost and Periglacial Processes, volume 28, pages 66-78. https://doi.org/10.1002/ppp.1880

Williams, P.L., and Smith, M.W., 1989. The Frozen Earth: Fundamentals of Geocryology; Cambridge University Press, Cambridge, United Kingdom, 306 pages.

Zoltai, S.C., and Tarnocai, C., 1975. Perennially Frozen Peatlands in the Western Arctic and Subarctic of Canada; Canadian Journal of Earth Sciences, volume 12, pages 28–43. https://doi.org/10.1139/e75-004

Zoltai, S.C., 1993. Cyclic Development of Permafrost in the Peatlands of Northwestern Canada; Arctic and Alpine Research, volume 25, number 3, pages 240–246. https://doi.org/10.2307/1551820